

Evaporation and rainfall interception data processing and analysis workshop.

M.J. Waterloo, R. Ronda, A. Meesters and A.J. Dolman



Amsterdam, November 2014



Cover page: Meteorological tower as set up in an abandoned agricultural field during the Portugal field course in June 2008

Contents

1	Introduction	4
1.1	Objectives	4
2	Energy balance and evaporation	6
2.1	Determining actual evaporation	6
2.1.1	Sensible heat flux	6
2.2	Soil heat flux	7
2.3	Penman open water evaporation	12
3	Workshop assignments	14
3.1	Selection of computer data analysis tools	14
3.2	Tools for the publication of your results	14
3.3	Organisation of your files	15
3.4	Before you start...	15
4	Assignment I: "dry" evaporation	16
4.1	Data description	16
4.2	Processing meteorological data and calculating actual evaporation	16
4.2.1	Reading data, assignment of variables and quality control .	16
5	Assignment II: "wet" evaporation	19
6	Reporting of results (optional!)	22
A	List of Symbols	26
B	Micrometeorological Formulae	28

Chapter 1

Introduction

1.1 Objectives

This document presents you with basic micrometeorological theory and related assignments. The theory covering the energy balance of the land surface is only partly given in the Ecohydrology course reader and the additional theory in this document also has to be studied for the exam. The assignments will be evaluated separately at the end of the workshops.

The objectives of the assignments presented in this document are to teach you how to process and analyse time series data that you obtain from meteorological and hydrological measurements in the field, and also to learn how to describe the results of data analysis in a report. This assignment can be subdivided into four parts:

- Calculation of several derived parameters from micrometeorological data, such as the energy balance components, [sensible heat flux H , soil heat flux G , latent heat flux λE ; ?] and potential evaporation estimates, such as Penman open water evaporation E_0 [Penman, 1956, 1963, Meyer, 1999, de Bruin and Kohsiek, 1981], Makkink evaporation or the FAO Penman Monteith reference evaporation,
- Learn how to calculate and model the above by computer programming with Python and how to use Python to plot and save professional-looking figures that you can use in a scientific report
- **Optional:** Learn how to model interception loss using the Gash Analytical model [Gash, 1979]. You will have to derive model parameters from measured rainfall and throughfall data (done in a spreadsheet program) and develop/program a function to model interception loss based on a rainfall time series (in Python),
- **Optional:** Learn how to report on evaporation, including rainfall interception, using images generated with your computer script and writing the ac-

companying descriptive text. Reporting may be done with \LaTeX , as an alternative to a word processor.

The measurement of meteorological parameters is thoroughly discussed by WMO [2008], including station layout, instrument accuracy and precision, measurement ranges, quality control and inter-calibration procedures. You are advised to read this document.

Note: The assignment has to be completed and handed in at or before the end of the last workshop in December.

Chapter 2

Energy balance and evaporation

2.1 Determining actual evaporation

Evaporation is often a very dominant component of the water balance. A few methods for measuring actual evaporation have been described in the ecohydrology reader. In this section theory will be presented about the energy balance and estimation of actual evaporation from micro-meteorological observations.

Under non-advective conditions the simplified energy balance of a vegetated surface may be written as:

$$\lambda R_n = \lambda E + H + G \quad (2.1)$$

where R_n is the net radiation, H the sensible-heat flux, λE the latent-heat flux and G the soil heat flux (all in W m^{-2}). Net radiation is normally measured with a net radiometer. In the sections below we will see how to determine the sensible heat flux H and soil heat flux G so that we can quantify λE from the energy balance.

2.1.1 Sensible heat flux

The absorption and transport of energy (heating or cooling) in the air above the land surface is a process that depends on vertical movements of the air due to the presence of eddies (turbulence). As such, the sensible heat flux can be measured with an eddy covariance technique, where measurements of the variations in vertical wind speed and corresponding variations in temperature are used. However, the equipment needed is very expensive and rather difficult to maintain.

Tillman [1972] showed that the standard deviation of high-frequency temperature measurements could also serve as a measure of the intensity of temperature fluctuations caused by turbulence. Based on this theory, Vugts et al. [1993] derived the following equation, relating the temperature (T) and its standard deviation (σ_T) to the sensible heat flux H :

$$H = \rho c_p \left[\left(\frac{\sigma_T}{C_1} \right)^3 \frac{kg(z-d)}{T} \right]^{\frac{1}{2}} \left(\frac{1 - C_2 \frac{z}{L}}{-\frac{z}{L}} \right)^{\frac{1}{2}} \quad (2.2)$$

where ρ is the density of air (kg m^{-3}), c_p the specific heat of air at constant pressure ($\text{J kg}^{-1} \text{K}^{-1}$), z the thermocouple measurement height (m) and d the displacement length (m). The acceleration due to gravity g is taken as 9.81 m s^{-2} , k is the *von Kármán constant* (set at 0.40) and the dimensionless constants C_1 and C_2 have generally accepted values of 2.9 and 28.4, respectively [De Bruin and van den Hurk, 1993]. The right hand term of this equation approaches to the value of C_2 in freely convective unstable atmospheric conditions when $C_2 z/L \gg 1$, *i.e.* with a Richardson number (a measure of atmospheric stability) below -0.1 [Wyngaard and Cote, 1971, Tillman, 1972]. Such conditions generally prevail between 0800 and 1700 h on dry sunny days. These conditions allow for a more simple approximation:

$$H = \rho c_p \left(k g (z - d) \frac{C_2}{C_1^3} \right)^{\frac{1}{2}} \left(\frac{\sigma_T^3}{T} \right)^{\frac{1}{2}} \quad (2.3)$$

The TVEB method combines the energy balance equation (Equation 2.1) with the sensible-heat flux equation (Equation 2.3) to derive estimates of λE under dry canopy conditions [De Bruin, 1982, Vugts et al., 1993]. The calculated λE includes energy used for transpiration, evaporation from the litter layer and soil evaporation.

2.2 Soil heat flux

When the surface of the Earth receives incoming short wave radiation during the day, its temperature increases rapidly and a temperature gradient develops between the surface soil layer and the layers below. This causes energy in the form of heat to diffuse into the soil, which is a positive ground heat flux. At night, the air above the surface cools down causing a decrease in the temperature of the surface soil layer. The layers below the surface layer now become warmer than the surface layer and an energy flux develops from the soil to the air. This is a negative ground heat flux.

The diffusion of heat into the soil occurs through molecular diffusion. Temperatures at a depth of only a few centimetres therefore usually vary already much slower than those in the surface layer. This implies that vertical temperature gradients in the topsoil are generally sharp and much stronger than any horizontal gradients of the soil surface temperature, which usually are averaged out efficiently due to the wind and turbulent exchange of heat at the soil–air interface. The energy flux G at a certain depth z into the soil column can be considered a first-order one-dimensional process, which can therefore be described by a one-dimensional diffusive flux equation (Fick's Law), analogous to the molecular transport of heat within solid bodies – Fourier's law of heat conduction:

$$G(z) = -\lambda_s \frac{\partial T_s}{\partial z} \quad (2.4)$$

where λ_s is the *thermal conductivity* or *heat conductivity* of the soil (a diffusivity constant) and $\partial T_s / \partial z$ is the gradient in soil temperature T with depth z . The minus

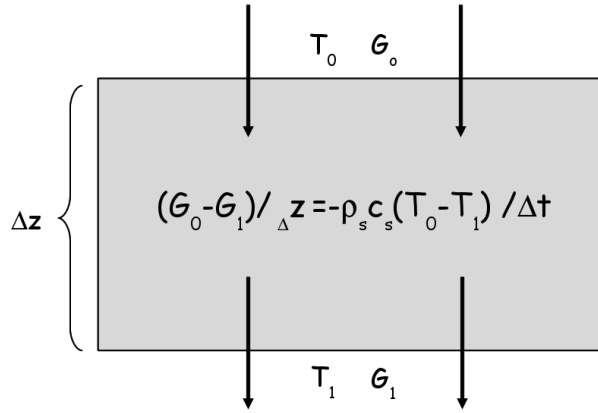


Figure 2.1: Schematic showing the soil heat flux in a infinitely thin layer of soil as driven by a temperature gradient.

sign appears in Equation 2.4 because the ground heat flux is in the direction of decreasing temperature. In principle, this equation can be used to determine the surface soil heat flux, but in practice it is very difficult to measure the thermal conductivity λ of the surface soil layer, where gradients in soil moisture content can be significant with depth.

The evolution of the temperature at a certain soil depth in time follows from the divergence of the flux, as given by Equation 2.4. A thin horizontal slab of dimension z that receives energy can take up part of the heat transported through the layer and releases heat to the next layer, leading to an increase of the flux through the layer with time t :

$$\rho_s c_s \frac{\partial T_s}{\partial t} = \frac{\partial G(z)}{\partial z} \quad (2.5)$$

where ρ_s is the *soil density* and c_s the *specific heat capacity* of the soil. The product of the density ρ_s and the specific heat capacity c_s is referred to as the *volumetric heat capacity*, denoted by $C_h = \rho_s c_s$. In finite difference form the process is depicted in Figure 2.1.

Soil consists of three components, *i.e.* solid material which is either mineral or organic, pore space filled with water and pore space filled with air. Each of these components has its own density, specific heat capacity and thermal conductivity. The volumetric heat capacity is represented by the average over all soil components, weighted by the fractions occupied by each component.

$$\rho_s c_s = \Sigma(f_i \rho_i c_i) \quad (2.6)$$

where ρ_i and c_i represent the density and volumetric heat capacity of each fraction i (air, water, mineral soil), respectively and f_i is the volume fraction of each component i . Table 2.1 summarizes typical values for the thermal conductivity, specific

heat capacity and density of common soil types at different moisture conditions. It also gives values for water, ice, snow and air. The volumetric heat capacity is larger for water than for solid mineral soil components (whereas it is negligible for air, due its low density).

Table 2.1: Representative values of the thermal conductivity λ , specific heat c_s and density ρ of soil for various types of surfaces (adapted from Table 11-3 in Pielke [2002]).

Material	λ [W m ⁻¹ K ⁻¹]	c_s [J kg ⁻¹ K ⁻¹]	ρ [kg m ⁻³]
Dry sand	0.15–0.25	800	1600
Saturated sand	2.20 – 4.00	1480	2000
Dry clay	0.15–0.25	890	1400
Saturated clay	0.60 – 2.50	1550	2000
Mineral quartz	1.30	670	2650
Kaolinite clay	0.34	1006	2600
Granite	1.7–4.0	790	2650–2750
Limestone	1.26–1.33	900	2100–2600
Rock	2–7	700–800	2700
Tuff (porous)	0.5–2.5	1000	1500–2500
Ice	2.50	2100	910
Old snow	1.00	2090	640
Fresh snow	0.10	2090	150
Water	0.60	4186	1000
Air	0.026	1006	1.2

Figure 2.2 shows the volumetric heat capacity as a function of the soil water content θ , *i.e.* the liquid water fraction of the soil. When the soil is completely dry ($\theta = 0$) the volumetric heat capacity takes on its lowest value determined mainly by the volumetric heat capacity of the mineral soil component. As the soil gets wetter and the air in the pores is gradually replaced by water, the volumetric heat capacity increases.

The thermal conductivity λ_s is not simply related tot the heat conductivities of the individual soil components, as in the case of the heat capacity. The conduction of heat occurs through sequences of conducting materials and the heat conductivity thus depends on how good conducting materials as quartz or clay minerals are interconnected, or whether they are separated by poorly conductive material, such as air in pores. Because water is a better thermal conductor than air, the heat conductivity λ varies as a function of the soil moisture content θ . Figure 2.2 shows the variation of heat conductivity with soil moisture content for a loam soil. When the soil is dry the heat conductivity is minimal. The transport of heat through the soil occurs through the narrow contact points of the solid soil particles. Initially, when the soil gets wet the increase in the thermal conductivity is only minor. Water

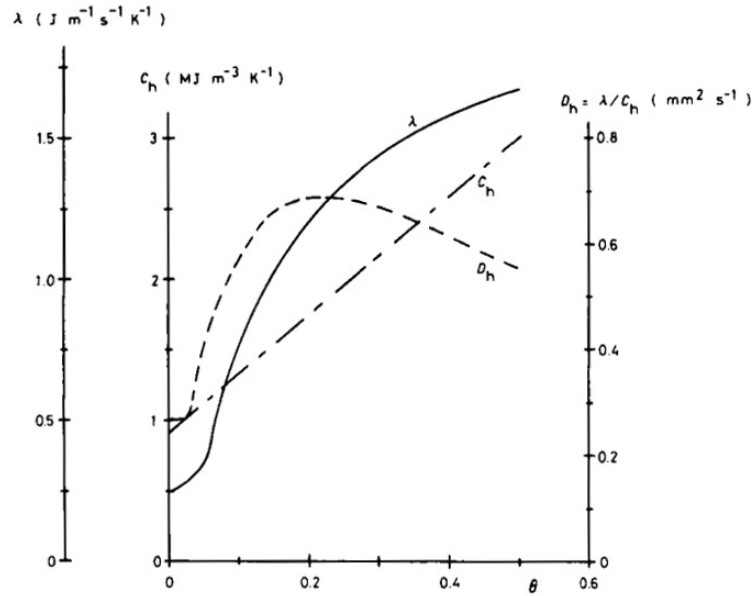


Figure 2.2: Thermal soil properties as a function of volumetric soil moisture content θ (source: Koorevaar et al. [1983]).

is present as thin films around the solid soil particles, which are not interconnected. As the soil moisture content further increases the gradually coarser pores fill with water through which heat can be conducted much more efficiently. Therefore, there is a sharp increase in the thermal conductivity as the soil get wetter and larger pores fill up. The maximum value of λ is reached when the soil is saturated.

Inserting Equation 2.4 that defines the ground heat flux $G(z)$ into Equation 2.5, which describes the evolution of the soil temperature in time, yields the Fourier equation:

$$\frac{\partial T_s}{\partial t} = D_h \frac{\partial^2 T_s}{\partial z^2} \quad (2.7)$$

where D_h is the *thermal diffusivity* of the soil, which is defined as:

$$D_h = \frac{\lambda}{C_h} \quad (2.8)$$

D_h is plotted as a function of the volumetric soil moisture content θ in Figure 2.2, together with the heat conductivity and capacity. Note the different sensitivity to soil moisture of the three parameters.

Analytical solutions of Equation 2.7 exist only for special cases. For instance, for a homogeneous soil where D_h is constant with depth, Equation 2.7 can be solved. The solution then depends on the prescribed boundary conditions. The simplest boundary condition is to assume that the variation of the surface tempera-

ture is given by a series of n sinusoidal functions (*e.g.* daily, seasonal, interannual):

$$T_s(z = 0, t) = T_a + \sum_{i=1}^n A_n \cos(\omega_i t) + B_i \sin(\omega_i t) \quad (2.9)$$

where A_i and B_i denote the amplitudes of the sinusoidal component with (angular) frequency $\omega_i = 2\pi i/P$, in which P denotes the longest period. For a diurnal variation ($P = 1$ day = 86400 s) $\omega = 2\pi/86400 = 7.27 \cdot 10^{-5} \text{ s}^{-1}$. The values of the amplitudes determine the importance of the sinusoid with frequency ω_i in the soil temperature. The most important frequency, which usually has the highest amplitude, is due to the daily cycle of the surface temperature caused by the diurnal pattern of the incoming short wave radiation. However, in the extra-tropics the surface radiation has also a strong seasonal cycle, implying that in these regions the period of one year ($P = 365$ days) is also important. Note that even slower frequencies can be observed due to variations in the solar constant (glacial periods). Higher frequencies also occur due to rapid fluctuation of the incoming short wave radiation due to the passage of clouds.

It can be shown that the solution of Equation 2.7 that matches surface condition defined by Equation 2.9 is:

$$T_s(z, t) = T_a + \sum_{i=1}^n \exp^{-\frac{z}{d_i}} \left[A_i \cos\left(\omega_i t - \frac{z}{d_i}\right) + B_i \sin\left(\omega_i t - \frac{z}{d_i}\right) \right] \quad (2.10)$$

in which d_i is the *damping depth*, the depth at which the amplitude of the sinusoidal function with ω_i has decreased to a value of $1/e$ times the amplitude at the surface. d_i can be calculated according to:

$$d_i = \sqrt{\frac{2D_h}{\omega_i}} = \sqrt{\frac{2\lambda}{\omega_i \rho_s c_s}} \quad (2.11)$$

Equation 2.11 implies that the damping depth is inversely proportional to the square root of the frequency. This means that components with a smaller frequency can penetrate much deeper into the ground than more rapid fluctuations. Using a value of $0.74 \cdot 10^{-6} \text{ m}^2 \text{ s}^{-1}$ the component with a frequency of one day will have a damping depth of about 0.14 m, while the component representing the seasonal cycle has a damping depth of about 2.7 m. This means that the temperature at shallow depths will be influenced by the daily variation in the surface temperature, whereas that deeper in the soil is only affected by a seasonal temperature cycle.

The ground heat flux as a function of time and depth can be found by differentiating Equation 2.10 to depth, and multiplying the resulting equation with the thermal conductivity λ . The final result of this complicated exercise is, for the surface ground heat flux (at $z = 0$):

$$G(0, t) = \lambda \sqrt{2} \sum_{i=1}^n \frac{1}{d_i} \left[A_i \cos\left(\omega_i t - \frac{\pi}{4}\right) + B_i \sin\left(\omega_i t - \frac{\pi}{4}\right) \right] \quad (2.12)$$

Comparing this equation with Equation 2.9, we note that the surface temperature $T(0, t)$ is delayed to the ground heat flux $G(0, t)$ with a phase shift of $\pi/4$. This implies that the heat flux in the diurnal cycle precedes the surface temperature by about 3 h on the daily and 1.5 month on the 365-days annual cycle.

If we now take the simple, but not unrealistic example of sinusoidal forcing, as might happen on a cloudless day with only direct radiation ($B = 0, i = 1$),

$$T(0, t) = T_a + A_1 \cos(\omega t) \quad (2.13)$$

with $\omega = 2\pi/P$ and P is one day, we obtain

$$T(z, t) = T_a + A_1 \exp^{-\frac{z}{d_1}} \cos\left(\omega t - \frac{z}{d_1}\right) \quad (2.14)$$

for the temperature variation with depth. The phase delay with respect to the surface is z/d_1 , and at $z = \pi d_1$ the phase will be completely opposite, while the maximum T occurs when $\omega t - z/d_1 = 0$ (see also Figure 3.6). A practical method to determine the damping depth and relevant soil parameters can be derived by observing maximum T_1, T_2 at times t_1, t_2 and depths z_1 and z_2 . This allows determination of the damping depth d_1 because:

$$t_1 - t_2 = \frac{z_1 - z_2}{\omega d_1} \quad (2.15)$$

When the damping depth d_1 has been established we can derive the other parameters from Equation 2.11.

For the simple sinusoidal forcing case, we obtain as the soil heat flux at the surface ($z = 0$) at a certain time t :

$$G(0, t) = A_1 \exp^{-\frac{z}{d_1}} \sqrt{\omega \lambda c_s \rho_s} \cos\left(\omega t - \frac{z}{d_1} + \frac{\pi}{4}\right) \quad (2.16)$$

A comprehensive review of different methods to estimate soil heat flux has been published by Sauer and Horton [2005].

For our exercise the soil heat flux at the surface is important and we have therefore measured the temperature gradient as close to the soil surface as possible. To do this we usually place temperature sensors at $z = 0.01$ and $z = 0.03$ m depth. Information about the thermal conductivity of different soil types and at different water contents is given in Table 2.1.

2.3 Penman open water evaporation

The Penman open water evaporation λE_0 (in W m^{-2}) has been developed by Penman [1956, 1963]) and may be calculated from daily average meteorological data as [de Bruin and Kohsiek, 1981]:

$$\lambda E_0 = \frac{\Delta R_n + \gamma \lambda E_a}{\Delta + \gamma} \quad (2.17)$$

where R_n represents the net radiation for an open water surface [W m^{-2}] and λE_a represents the aerodynamic evaporation [W m^{-2}]. The input of net radiation [W m^{-2}] for an open water surface is given by:

$$R_n = R_s \downarrow (1 - \alpha) - R_{ln} \quad (2.18)$$

where R_s is the incoming short-wave radiation [W m^{-2}], α the albedo of open water (0.06) and R_{ln} the net-longwave radiation [W m^{-2}]. The latter can be obtained from:

$$R_{ln} = \sigma T_2^4 (0.53 - 0.67\sqrt{e_2})(0.2 + 0.8n/N) \quad (2.19)$$

where σ is the Stefan-Boltzmann constant ($5.670 \cdot 10^{-8} \text{ W m}^{-2} \text{ K}^{-4}$), T is the daily average air temperature (K), e is the average daily water vapour pressure of the air (hPa), n is the duration of bright sunshine (h), N is the maximum possible sunshine duration [de Bruin and Kohsiek, 1981, h;]. The aerodynamic term E_a [W m^{-2}] is a function of the wind speed and vapour pressure deficit [de Bruin and Kohsiek, 1981].

$$\lambda E_a = (3.7 + 4.0u_2) \cdot (e_s(T_2) - e_2) \quad (2.20)$$

where u_2 is the wind speed (m s^{-1}), $e_s(T_2)$ the saturation vapour pressure [hPa] at air temperature T [K] and e_2 the actual vapour pressure [hPa]. Conventionally, all micrometeorological parameters should be measured at a height of 2 m above ground level.

The maximum possible sunshine duration N for a certain location can be looked up in tables and amounts to 14.5 h for this site in June. We have not measured the actual sunshine duration n . However, the following empirical relation exists between n/N , R_s and the solar radiation received at the top of the atmosphere R_{ext} [Rietveld, 1978]:

$$R_s = (0.24 + 0.50n/N)R_{ext} \quad (2.21)$$

We can easily invert this equation to get n , using daily solar radiation input R_s ($\text{MJ m}^{-2} \text{ day}^{-1}$), N and R_{ext} . The latter amounts to $41.16 \text{ MJ m}^{-2} \text{ day}^{-1}$. Note that n cannot be less than zero hours.

The crop factor f can be calculated as the fraction of the actual and reference evaporation values.

Note that the Penman evaporation is available in the *evaplib.py* module.

Chapter 3

Workshop assignments

3.1 Selection of computer data analysis tools

Although the assignments can all be done in a spreadsheet program, we do prefer that you do some of these assignments in *Python* to learn the logic of programming at the same time, and to create professionally looking images. The Python script files (.py) files that you develop here can also very easily be used for analysing meteorological data collected during the field courses in Twente and Portugal, which will save you a lot of time later in your MSc programme. In addition, these script files can also easily be adapted when you have to process other time series data. To teach yourself Python, please visit the <http://python.hydrology-amsterdam.nl/> web page and download the Python tutorial and example script files. Please do read the manual before you start the exercises! At the end of the course you will have to hand in your complete and functioning Python scripts.

3.2 Tools for the publication of your results

As an option if you have time left, the outcome of the assignments could be given in the form of a short report, preferably made in \LaTeX . Unlike word processors (*e.g.* OpenOffice Writer, MS-Word), \LaTeX is a typesetting system that was specifically designed for the production of technical and scientific documentation, and is used to typeset papers by many of the scientific journals. The advantage of \LaTeX over word processors is that it will handle the layout for you, according to professional typographic standards for document publishing. This leads to documents that are well-structured and with layouts that are easy to read. This document has been produced with \LaTeX .

A document with guidelines for writing a scientific paper, templates for BSc, MSc and PhD reports and instructions for getting and installing \LaTeX on your computer are given at <http://thesistools.hydrology-amsterdam.nl/index.html>. Please check the <http://thesistools.hydrology-amsterdam.nl/index.html> site for information on how to use \LaTeX to prepare a report. A \LaTeX template file (assign-

ments.tex) is available on Blackboard to help you create a very professional report.

3.3 Organisation of your files

Before you can start, you have to download several files that we need for the assignments. Organizing these in several sub-directories will help you find the files back later. Organizing your data in a structured way will be even more important when you get a large amount of data from different measurements, such as made during field campaigns.

Please start by making a directory */ecohydrology*, which will hold all your sub-directories. We advise you to do this on a USB memory stick so that you do not have to leave your data on a VU computer where it is less safe. As an alternative you can use your VU network drive, which has limited storage space. In the */ecohydrology* directory, create the following sub-directories:

- */data*, which will hold the *slowtable.dat* file with the half-hourly meteorological data stored by our Campbell CR1000 data logger. Please download this file from Blackboard.
- */pyscripts*, which will hold your python scripts and function library files. Download the *meteoscript_yourname_2014.py* script file from Blackboard and the *meteolib.py* and *evaplib.py* function library files from the Python page at <http://python.hydrology-amsterdam.nl>
- */report*, which holds your report files.
- Within the *ecohydrology/report* subdirectory create */images* and */library* sub-directories, these are for storing image files (made with Python) and your literature reference library file, respectively.
- Finally, make a directory called *presentation* where you will develop the presentation about an ecohydrological paper that you need to give at the end of this course.

3.4 Before you start...

For the assignments below you need some basic knowledge of Python. You should therefore read the python manual and study the script file that goes with it. Make sure that you have done this before the Python workshop starts! In addition, you will need basic knowledge about evaporation formulae and rainfall interception measurement and modelling. This information is given in the Ecohydrology course reader. Below you will find some information on a method for determining actual evaporation of an area. This information is not presented in the course reader but is part of the ecohydrology exam.

Chapter 4

Assignment I: "dry" evaporation

4.1 Data description

We shall be working with meteorological data collected by hydrology students during the field course Portugal in 2014. The meteorological tower was placed on an abandoned agricultural field, of which the soil (fine sand) was covered with grass of about 40 cm height. A photograph of the tower setup is shown on the cover of this document. A description of the instruments used and their installation heights is given in Table 4.1.

4.2 Processing meteorological data and calculating actual evaporation

4.2.1 Reading data, assignment of variables and quality control

In this section you will practise how to calculate daily averages from half-hourly values and plot data to provide graphical representations of data in your report. We start with reading the data from file and preparation of graphs showing time series of different meteorological variables.

- a. Start up *Idle* or *Spyder* from Python(x,y) and open the *meteoscript_yourname_2014.py* file that you downloaded before. This is the Python script file that we will use for this assignment. First, save the file as *meteoscript_yourlastname_2014.py*.
- b. The script file already loads a few function modules and contains comments and tips for doing the assignments. Please note that a number of statements have been commented out (using the # symbol) and you will have to remove these comments during the exercise. You can already run the script in *Spyder* and you will see some printouts being generated and a few empty images. Throughout the script you will find instruction on what to do.

Table 4.1: Description of the data in the *slowtable.dat* file, the instruments used and the units corresponding to the data. The first column is the date and time set by the data logger during the measurement, whereas the last column represents the rainfall data. The codes in this table can be used to name the column variables in Python.

Parameter	Instrument manufacturer, type and country	Code	Unit	Height (m)
ID number	-	ID	-	-
Year	-	year	-	-
Julian day	-	doy	-	-
Time	-	time	-	-
Datalogger temperature	Campbell 21X	Tpanel	°C	0.40
Net radiation	REBS Q*7, USA	Rnet	W m ⁻²	1.60
Incoming radiation	Skye 1411, USA	Rin	W m ⁻²	1.70
Relative humidity	Vaisala HMP35, Finland	vaisRH	%	2.90
Air temperature	Vaisala HMP35, Finland	vaisT	°C	2.90
Air barometric pressure	VUA, Netherlands	Airpress	hPa	0.40
Thermocouple dry (average)	VUA, Netherlands	TCavg	°C	2.60
Thermocouple dry (variance)	VUA, Netherlands	TCvar	°C	2.60
Thermocouple dry (standard deviation)	VUA, Netherlands	TCstd	°C	2.60
Thermocouple soil temperature	VUA, Netherlands	TCsoil1	°C	-0.01
Thermocouple soil temperature	VUA, Netherlands	TCsoil3	°C	-0.02
Windvector speed	Vector Instruments A101ML, USA	U	m s ⁻¹	2.95
Windvector direction	Vector Instruments W200P, USA	winddir	° N	2.95
Rainfall	VUA, Netherlands	P	mm	0.80
Soil moisture content	CS616, Campbell Scientific	theta	%	0 – -0.30 m
Soil moisture content	CS616, Campbell Scientific	theta	%	-0.3 – -0.6 m
Soil moisture content	CS616, Campbell Scientific	theta	%	-0.6 – -0.9 m
Ground water level (not connected)	Druck, USA	gw1	m	-3.5
Battery voltage	-	Vbatt	V	0.40

- c. Note that you will also find lines with questions (marked by #Q1, #Q2, etc.) throughout the script. Please write down the answers to these questions as comments below the question in the script.

Using the above theory and equations, we are going to calculate the actual evaporation with the measurements made in Portugal. Formulae for the different parameters in the equations and quantities like e_s are given in Appendix B.

To make things easy, I have developed a meteorological function library for Python, with functions to calculate different meteorological parameters, such as saturated water vapour pressure e_s , γ , λ , etc. These functions are defined in the *meteolib.py* library. Please download these modules from <http://python.hydrology-amsterdam.nl/index.html> and save these in the same directory where your script resides. The functions are based on the formulae given in Appendix B.

Follow the instructions in the script to finish the assignment.

Chapter 5

Assignment II: "wet" evaporation

For this assignment there are two options.

I Friso Holwerda of our Department of Hydrology and Geo-Environmental Sciences has been measuring interception losses in a lowland rain forest in Puerto Rico by varying approaches. In one instant, he used 60 fixed gauges to measure throughfall. The data for 29 storm events in November and December 2000 are given in the sheet *interception_data*. Stemflow data have not been added here but indicated that the fraction of rainfall going to the stems was 2.3%, while stem storage can be neglected. Use the information in the following assignments.

- (a) Using the data of all 60 gauges, calculate the following statistics in a spreadsheet:
 - a. Total rainfall, throughfall and stemflow for this period
 - b. Interception losses (in mm for the whole period, mm per storm, and as a percentage of rainfall).
 - c. The total throughfall measured in each gauge (gauge catch) as a percentage of rainfall. Construct a graph similar to those in Fig. 5.5a in Chapter 5 in the reader, but using 20% intervals.
 - d. What is the highest gauge catch? Can you explain it?
 - e. How does interception loss (%) change if you leave this gauge out of the data?
- (b) One of the purposes of collecting this data set was to compare the use of a fixed number of gauges with roving gauges. Answer the following questions:
 - a. At random pick six out of the sixty gauges. What would be the estimated interception losses (in %) if you had you would have only used these gauges? Assume that the 60 gauges provide a best estimate of interception losses. What is the error (difference, in % of rainfall) in the six-gauge estimate compared to this best estimate?

- b. Repeat this four more times and calculate the average and range of resulting interception percentages and errors.
 - c. To some extent, you can simulate measurements with a limited number of roving collectors by taking using the values of different fixed gauges for every sampling occasion. An example with six roving gauges is shown in sheet *exercise II*. Is the resulting interception estimate closer to the best estimate?
 - d. Now assume that the catch at position 22 indicated bold (cell X26) did not occur, but that the gauge was placed at position 21. Is the estimate better in this case? What does this tell you about fixed and roving throughfall gauge measurements?
- (c) Rainfall, the best-estimate throughfall, estimated stemflow and resulting interception losses are calculated in sheet *exercise III*.
- a. Negative interception losses seem to occur on some days. Give two explanations for this (apparent) phenomenon.
 - b. Using the method of Leyton et al. [1967] (see reader Chapter 5, p.5-20) determine the value of canopy storage capacity S . Use only storms above an (arbitrary) threshold P_G of 2 mm. Is the resulting S realistic? What assumptions underlying the used regression method may be violated here?
 - c. Following the method used by Gash and Morton [1978] (p.5-21) estimate the free throughfall coefficient p . Do this for values of threshold P_G of 1.0 and 2.0 mm, respectively. Does this result in realistic p values, given that the rain forest has a nearly closed canopy? What may explain this?

II Interception modelling with the analytical interception model Gash and Morton [1978]. In this exercise we are switching to Python to write a function that calculates interception losses. Model the measured interception losses with the original analytical interception model of Gash [1979] (Table 5.1 in Chapter 5 of the ecohydrology reader).

- a. Open a new file in Spyder (or Idle) to develop a new script, a skeleton script is available on Blackboard for this purpose. Use routines from the meteorology script to import the daily rainfall file and assign variables to the date and rainfall P_G . A data file for a heath forest is also available on Blackboard.
- b. Now write a Python function that uses the rainfall and a set of Gash parameters to calculate interception loss, throughfall and stemflow. You can see how to define a function in the Python manual, and there are examples in `meteolib.py` and `evaplib.py`.
- c. Write the results to a text file (see Python manual).

- d. When you have your script ready, read the rainfall input file and run the model using the model parameter values based on an model application by Schellekens et al. [2000]. He observed values of: $\overline{E}/\overline{R} = 0.51$; $p = 0.23$; $S = 1.15$ mm; $p_t = 0.023$ and $S_t = 0$. (Note that because $S_t = 0$, stem evaporation is also zero). Plot the cumulative values of measured and modelled interception loss. Judging this graph, what can you say about model performance?
- e. Micrometeorological measurements by Schellekens et al. [2000] actually suggested a value of $\overline{E}/\overline{R} = 0.06$, but in his case this did not give a good model fit. Use this value instead. Does model fit get better or worse?
- f. When looking at the high density of the rain forest canopy, $p = 0.05$ may be a more realistic value. Does model fit get better or worse?
- g. Also, actual canopy storage may well be different than the 1.15 mm used. Adjust the value of S to get a better fit. In what value does this result? Compare this with values listed in Table 9 of the paper by van Dijk and Bruijnzeel [2001]. Discuss whether the resulting S value compares well with these literature values, and if not, provide possible explanations.

Chapter 6

Reporting of results (optional!)

A very important aspect of data analysis is the subsequent reporting of the results in a scientific report or as a paper in a journal. A template for an article about the meteorological data is given on Blackboard (`_meteo_report_template.tex`) and should be downloaded to the *report* directory. This template already contains an unfinished abstract, a short introduction, a description of the measurement methods and theory and some entries for you to complete. If you want and have time, you could place your images in the results section and describe your findings as a practice for report writing in the Portugal field course. The description should include information about the general weather trends in the study period, diurnal patterns (cloudy/sunny days), a table with daily averages, etc.

Due to time limitations, this is now an optional part of the workshop. If you finish the previous assignments early that you can gain a bonus point for doing the reporting.

Bibliography

- Richard G. Allen, Luis S. Pereira, Dirk Raes, and Martin Smith. *Crop evapotranspiration – Guidelines for computing crop water requirements*, volume 56 of *FAO Irrigation and Drainage Papers*. FAO, Rome, 1998. URL <http://www.fao.org/docrep/X0490E/x0490e00.htm>.
- J. Bringfelt. Test of a forest evapotranspiration model. *Meteorology and Climatology Reports* 52, SMHI, Norrköpping, Sweden, 1986.
- H. A. R. De Bruin. *The energy balance of the earth's surface: a practical approach*. PhD thesis, Wageningen Agricultural University, Wageningen, The Netherlands, 1982.
- H.A.R. de Bruin and W. Kohsiek. Toepassingen van de Penman formule. Wetenschappelijk Rapport WR 79-3, Koninklijk Nederlands Meteorologisch Instituut (KNMI), De Bilt, The Netherlands, 1981. URL <http://www.knmi.nl/bibliotheek/knmipubWR/WR79-03.pdf>. Applications of the Penman equation.
- Kohsiek W. De Bruin, H. A. R. and B. J. J. M. van den Hurk. A verification of some methods to determine the fluxes of momentum, sensible heat and water vapour using standard deviation and structure parameter of scalar meteorological quantities. *Boundary-Layer Meteorology*, 63:231–257, 1993.
- J. H. C. Gash. An analytical model of rainfall interception by forests. *Quarterly Journal of the Royal Meteorological Society*, 105:43–55, 1979.
- J. H. C. Gash and A. J. Morton. An application of the Rutter model to the estimation of the interception loss from Thetford Forest. *Journal of Hydrology*, 38:49–58, 1978.
- J.A. Goff. Saturation pressure of water on the new Kelvin temperature scale. In *Transactions of the American Society of Heating and Ventilating Engineers*, pages 347–354, Murray Bay, Quebec, Canada, 1957. Presented at the semi-annual meeting of the American Society of Heating and Ventilating Engineers.
- P. Koorevaar, G. Menelik, and C. Dirksen. *Elements of Soil Physics*, volume 13-XIV of *Developments in Soil Science*. Elsevier Science Ltd., Amsterdam, November 1983.

- L. Leyton, E. R. C. Reynolds, and F. B. Thompson. Rainfall interception in forest and moorland. In *International Symposium on Forest Hydrology*. Pergamon Press, Oxford, 1967.
- W. S. Meyer. Standard reference evaporation calculation for inland, south eastern Australia. Technical Report 35/98, CSIRO Land and Water, Adelaide Laboratory, Adelaide, Australia, September 1999. URL <http://www.clw.csiro.au/publications/technical98/tr35-98.pdf>.
- H. L. Penman. Evaporation: An introductory survey. *Neth. J. Agric. Sci.*, 4:9–29, 1956.
- H. L. Penman. Vegetation and hydrology. Technical communication 53, Commonwealth Agricultural Bureaux, Farnham Royal, Bucks, UK, 1963.
- R.A. Pielke. *Mesoscale meteorological modeling*. International geophysics series. Academic Press, 2002.
- M. R. Rietveld. A new method for estimating the regression coefficients in the formula relating solar radiation to sunshine. *Agricultural Meteorology*, 19:243–252, 1978.
- T.J. Sauer and R. Horton. *Soil heat flux*, volume 47, agronomy monograph 7, pages 131–154. American Society of Agronomers, Crop Science Society of America, Soil Science Society of America, USA, 2005. URL <http://ddr.nal.usda.gov/bitstream/10113/28089/1/IND44188416.pdf>.
- J. Schellekens, L. A. Bruijnzeel, F. N. Scatena, N. J. Bink, and F. Holwerda. Evaporation from a tropical rain forest, Luquillo Experimental Forest, eastern Puerto Rico. *Water Resources Research*, 36(8):2183–2196, 2000. URL <http://flow.geo.vu.nl/papers/wrr36.pdf>.
- J. E. Tillman. The indirect determination of stability, heat and momentum fluxes in the atmosphere boundary layer from simple scalar variables during dry unstable conditions. *Journal of Applied Meteorology*, 11:783–792, 1972.
- A. I. J. M. van Dijk and L. A. Bruijnzeel. Modelling rainfall interception by vegetation of variable density using an adapted analytical model. part 2. model validation for a tropical mixed cropping system. *Journal of Hydrology*, 247:239–262, 2001.
- H. F. Vugts, M. J. Waterloo, F. J. Beekman, K. F. A. Frumau, and L. A. Bruijnzeel. The temperature variance method: a powerful tool in the estimation of actual evaporation rates. In J. S. Gladwell, editor, *Hydrology of Warm Humid Regions, Proc. of the Yokohama Symp.*, IAHS Publication No. 216, pages 251–260, July 1993.

WMO. Guide to meteorological instruments and methods of observation. WMO Report 8, World Meteorological Organization, Geneva, Switzerland, 2008. Seventh edition.

J. C. Wyngaard and O. R. Cote. The budgets of turbulent kinetic energy and temperature variance in the atmospheric surface layer. *Journal of Atmospheric Sciences*, 28:190–201, 1971.

Appendix A

List of Symbols

The following list gives a short description of the symbols with their units.

Symbol Description and unit

β	Bowen ratio
c_p	Specific heat of air at constant pressure [$\text{J kg}^{-1} \text{K}^{-1}$]
γ	Psychrometric constant [hPa K^{-1}]
d	Zero plane displacement length [m]
Δ	Change of the saturation vapour pressure with temperature [hPa K^{-1}]
e	Water vapour pressure in air [hPa]
e_s	Saturation vapour pressure of air [hPa]
G	Flux density of heat into the soil [W m^{-2}]
g	Gravitational acceleration [9.81 m s^{-2}]
H	Sensible heat flux [W m^{-2}]
h	Mean vegetation height [m]
k	Von Karman's constant, 0.4
λ	Latent heat of vapourization of water [J kg^{-1}]
λE	Latent heat flux [W m^{-2}]
n	Sample size
P	Rainfall total [mm]
q	Specific humidity of air [kg m^{-3}]
$R_s \downarrow$	Incoming short-wave radiation [W m^{-2}]
RH	Relative humidity [%]
R_n	Net radiation [W m^{-2}]
r_a	Aerodynamic resistance [s m^{-1}]
ρ	Density of air [kg m^{-3}]
T	Temperature [$^{\circ}\text{C}$, K]
t	Time [s; h; day; year]
$u(z)$	Wind speed at height z above the soil surface [m s^{-1}]

z Height above the surface [m]
 z_0 Aerodynamic roughness length [m]

Appendix B

Micrometeorological Formulae

In this section the formulas used for the calculation of micrometeorological constants, as well as those used to calculate parameters dependent on temperature and relative humidity will be presented. The following formula [Goff, 1957] was used to calculate the saturated vapour pressure (e_s , in hPa) from the temperature (T , in K):

$$e_s = 10^{10.79574\left(1-\frac{T_0}{T}\right) - 5.028 \log\left(\frac{T}{T_0}\right) + 1.50475 \cdot 10^{-4} \left(1 - 10^{-8.2969\left(\frac{T}{T_0}-1\right)}\right) + 0.42873 \cdot 10^{-3} \left(10^{4.76955\left(1-\frac{T_0}{T}\right)} - 1\right) + 0.78614} * 10$$

where T_0 is 273.15 K.

A much simpler formula [Allen et al., 1998]:

$$e_s = 6.108 \exp\left(\frac{17.27T}{237.3+T}\right)$$

where e_s is again in hPa and T in °C.

The actual vapour pressure e can be obtained from e_s and the relative humidity (RH, in %):

$$e = \frac{RH}{100} \cdot e_s$$

The specific humidity of the air (q , in kg m^{-3}) can be approximated by:

$$q = 0.622 \cdot \frac{e}{p - 0.378e}$$

where p was set at 998 hPa.

The slope of the saturated vapour pressure curve (Δ , in hPa K^{-1}) is obtained

by differentiating the equation used to calculate e_s with respect to T [WMO, 2008]:

$$\begin{aligned}\Delta &= \frac{de_s}{dT} \\ &= e_s \cdot \left[\frac{10.79574T_0}{0.4343T^2} - 5.028 \frac{1}{T} \right. \\ &\quad + 1.50475 \cdot 10^{-4} \frac{8.2969}{0.4343^2 T_0} \cdot 10^{8.2969 \left(1 - \frac{T}{T_0}\right)} \\ &\quad \left. + 0.42873 \cdot 10^{-3} \frac{4.76955T_0}{0.4343^2 T^2} \cdot 10^{4.76955 \left(1 - \frac{T_0}{T}\right)} \right]\end{aligned}$$

For the simpler formula, the differentiation of the equation for e_s gives:

$$\Delta = \frac{5420.32}{(T + 273.15)^2} e^{21.6562 - \frac{5420.32}{T + 273.15}}$$

where T is again in °C.

The latent heat of vapourization (λ , in J kg⁻¹) is dependent on the temperature (T , in K) and was calculated as follows [Bringfelt, 1986]:

$$\lambda = 4185.5 \cdot (751.78 - 0.5655T)$$

The specific heat of air (c_p , in J kg⁻¹ K⁻¹) from e , where the atmospheric pressure p was assumed constant at 998 hPa:

$$c_p = 0.24 \cdot 4185.5 \left(1 + 0.8 \frac{0.622e}{p - e} \right)$$

The density of the air (ρ , in kg m⁻³) fluctuates with the temperature (T , in K), vapour pressure (e , in hPa) and pressure (p , set at 998 hPa) of the air and can be calculated from the following expression:

$$\rho = 1.201 \frac{290 \cdot (p - 0.378e)}{1000T}$$

The psychrometric constant γ [hPa °C⁻¹] was calculated as [Bringfelt, 1986]:

$$\gamma = \frac{c_p \cdot p}{0.622 \cdot \lambda}$$

where p is the air pressure in hPa and c_p and λ are as defined above.